Heavy neutrino searches via same-sign lepton pairs at a Higgs boson factory

Yu Gao[1,*] and Kechen Wang[2,†]

[1]*Key Laboratory of Particle Astrophysics, Institute of High Energy Physics, Chinese Academy of Sciences, Beijing 100049, China*
[2]*Department of Physics, School of Science, Wuhan University of Technology, 430070 Wuhan, Hubei, China*

This paper investigates the $e^-e^+ \to Zh_1$ sensitivity for a Higgs boson's rare decay into heavy neutrinos $h_1 \to NN$ at the proposed electron-positron collider, with the focus on multilepton final states that contain same-sign lepton pairs. $h_1 \to NN$ decay can derive from Higgs bosons mixing with new physics scalar(s) in a way that is complementary to the contribution from active-sterile neutrino mixings. We consider the scenario with a singlet scalar that gives the heavy neutrino mass and has a small mixing with the SM Higgs boson. We analyze the semileptonic, fully leptonic, and mixed NN decay scenarios, and we categorize the signal based on the number of leptons in the final state: $\ell^\pm \ell^\pm$ with at least three jets, $\ell^\pm \ell^\pm \ell$ with at least two jets, and $e^\pm e^\pm \mu^\mp \mu^\mp$ with at least one jet, each containing one or two same-sign dilepton system(s). Selection cuts are optimized for the presence of the associated Z boson, which leads to additional backgrounds at the e^-e^+ collider. The Standard Model background channels are systematically analyzed. Sensitivity limits on $h_1 \to NN$ branching fractions are derived for signals with two to four final leptons, assuming the heavy neutrino masses are between 10 and 60 GeV. With 240 GeV center-of-mass energy and 5.6 ab^{-1} design luminosity, the $h_1 \to NN$ branching fraction can be probed to 2×10^{-4} in the 2ℓ and 3ℓ channels, and to 6×10^{-4} in the 4ℓ channel at a 95% confidence level. The 3ℓ and 4ℓ channels expect one background event or fewer, and their sensitivities saturate the statistic limit at 5.6 ab^{-1} luminosity. A same-sign trilepton ($\ell^\pm \ell^\pm \ell^\pm$) signal in the 3ℓ channel is also discussed. Our search strategy provides an approach to discovering the singlet scalar and exploring the origin of neutrino masses at future e^-e^+ colliders.

I. INTRODUCTION

The collider search for massive neutrinos plays an important role in the testing of neutrino mass models based on the seesaw mechanism [1–5]. The mass of the active neutrino ν is generated by mixing the left-handed neutrino (ν_L) of the Standard Model (SM) with the additional right-handed neutrino N_R, resulting in a heavy mass eigenstate N that has a small SM ν_L component. The heavy N acquires effective couplings to the SM model gauge bosons via its weakly charged ν_L component [6] and is extensively searched at colliders. See the review in Refs. [7,8] and references therein for collider searches of

heavy neutrinos. Experimental limits can be found in Refs. [9–14].

Recent phenomenology studies on heavy neutrino searches at e^-e^+ colliders vary according to their different production and decay channels. For the prompt decays of heavy neutrinos, searches have been investigated under the symmetry-protected seesaw model in Refs. [15–17] and the EFT framework in Ref. [18]; heavy neutrinos from the production process $e^-e^+ \to \nu N$ are studied at center-of-mass energy $\sqrt{s} = 240$ GeV [19] and Z-pole running mode [20,21]; Ref. [22] considers the N production from B-meson decays $B^+ \to \mu^+ N \to \mu^+ \mu^+ \pi^-$, while Refs. [23,24] consider the lepton-number-violating final state for the Majorana N from the process $e^-e^+ \to \ell^\pm W^\mp N \to \ell^\pm \ell^\pm + 4j$. For the displaced vertex searches of long-lived N, Refs. [25,26] consider the production from $e^-e^+ \to \nu N$, while Ref. [27] considers the production from tau decays at B factories. Furthermore, limits have also been set indirectly based on the N's corrections to the decay branching ratio of the Z boson into two leptons $\mathrm{Br}(Z \to \ell_1^\mp \ell_2^\pm)$ at Z-pole running mode [28], and to the cross section of the SM

Higgs boson production process $e^-e^+ \to W^-W^+h_1$ at $\sqrt{s} = 3$ TeV [29].

While the heavy N_R mass scale explains the tiny active neutrino mass, it also suppresses the left-right neutrino mixing and makes the weak production of heavy neutrinos difficult when this mixing is small. Alternatively, heavy neutrinos can also be produced in case they couple to beyond-the-Standard Model (BSM) mediators—e.g., extra gauge bosons or scalars that couple to SM particles. Currently, such BSM gauge bosons are stringently constrained by resonance searches [30,31] and electroweak precision data [32,33]. In comparison, a mixing between Higgs bosons with BSM singlet scalar(s) is less constrained [34], and it is among the major physics goals at future Higgs factories [35,36].

The right-handed neutrino can obtain its mass by coupling to BSM scalars with a nonzero vacuum expectation value (VEV). Generally, such scalars mix with the SM Higgs doublet scalar, so if kinematically allowed, the physical Higgs boson can decay into heavy neutrinos through its BSM component. Since this decay occurs directly through the scalar mixing, it is insensitive to $\nu_L - N_R$ mixing, and thus it is complementary to $|V_{\ell N}|^2$-based searches. Typical implementations involve extending the SM's scalar sector—e.g., from UV-complete models such as left-right symmetric models [37], $U(1)_{B-L}$ models [3], next-to-minimal supersymmetric models [38], or alternatively, rising from effective theory operators [39], fourth-generation neutrinos [40], etc.

When the Higgs boson decays into heavy neutrinos $h_1 \to NN$, a rare multilepton Higgs decay emerges. N subsequently decays to SM particles through its ν_L component's weak interaction. The fully leptonic $N \to \ell\ell'\bar{\nu}$ and semileptonic $N \to \ell jj$ channels are interesting i collider searches due to the presence of measurable charged leptons in the final state. When N is a Majorana fermion, semileptonic NN decay leads to the characteristic lepton-number-violating (LNV) same-sign (SS) dilepton, recently studied as a LNV probe for Higgs-BSM scalar mixing [41–44].

For collider searches, increased lepton multiplicity and the existence of SS lepton pairs greatly reduce the SM's background, particularly for hadron collisions. In our previous work [45], we demonstrate that a characteristic signal of two same-sign, same-flavor (SSSF) lepton pairs plus missing energy from the NN decay can probe the Higgs-singlet mixing with high precisions at the current and future pp colliders. At lepton colliders, in comparison, hadronic backgrounds are controllable, and the dominant Higgs boson production is the $e^-e^+ \to Zh_1$ channel.

The associated Z boson always appears, and it provides additional leptons or jets to the final state. This is a complication at the lepton collider. Lepton colliders are known for high sensitivity to relatively soft leptons, yet intrinsic multitau backgrounds for SS dileptons do exist.

Thus, it is of interest to systemically study the multilepton sensitivity at future lepton colliders, and we will show that the associated Z boson leads to both signal and extra background. In addition, a characteristic SS trilepton signal emerges, unique to the dominant Zh_1 channel at the e^-e^+ Higgs factory. In this consecutive work, according to the semileptonic, fully leptonic, and mixed NN decays, we categorize the signal based on the number of final-state leptons at future e^-e^+ colliders. After simulating the signal and SM background processes and performing the data analyses, we forecast the sensitivity limits on $h_1 \to NN$ branching fractions for signals with two to four final leptons, assuming the heavy neutrino masses are between 10 and 60 GeV. Our signal channels at both pp and e^-e^+ colliders provide approaches to discovering the singlet scalar and exploring the origin of neutrino masses.

The proposed lepton collider missions—e.g., the CEPC [46], ILC [47], and FCC-ee [48]—are designed to yield $\mathcal{O}(10^{6-7})$ Higgs events. Any Higgs decay branching limit would be statistically capped by the collider's luminosity inverse. This study on the relevant backgrounds would also help in understanding whether future $h_1 \to NN$ sensitivity would saturate luminosity limits.

This paper is organized as follows: Sec. II briefly discusses a minimal singlet extension to the SM that implements the $h_1 \to NN$ decay channel. Sections III to V categorize signal channels based on the number of final-state leptons, analyzing each channel's SM background and the event selection strategies. In Sec. VI, we give the sensitivity limits at a future Higgs factory.

II. MODEL SETUP

For collider search purposes, we adopt the phenomenological simple extension to the Standard Model that implements a type-I seesaw mechanism. With a scalar S and a Majorana fermion N_R that are both SM gauge singlets, the addition to the interaction Lagrangian is given by

$$\mathcal{L} \supset y_D \bar{L} \tilde{H} N_R + y_S S \bar{N}_R^C N_R + \text{H.c.}$$
$$+ \frac{\lambda}{2} |H|^2 |S|^2 + V_S, \tag{1}$$

where $\tilde{H} = i\sigma_2 H^*$, and H is the SM Higgs doublet, y_D and y_S are the couplings that give the Dirac and Majorana mass terms after the doublet H and the singlet S obtain their vacuum expectation values of $v_H = 246$ GeV and v_S. The light neutrino mass eigenstate(s) obtain a mass $m_\nu \sim y_D^2 v_H^2/(y_S v_S)$, and the left-right neutrino mixing parameter $|V_{\ell N}| \sim \sqrt{m_\nu/m_N} = y_D v_H/(y_S v_S)$ is quite tiny for v_S at weak scales or higher. The smallness of $|V_{\ell N}|$ thus suppresses the massive eigenstate N's effective couplings [6] to weak gauge bosons as $|V_{\ell N}|^2 \sim m_\nu/m_N$. Here we adopt this singlet scalar extension for its phenomenology simplicity: it is a low-cost extension to the SM that allows

us to have an uncharged scalar around the weak scale that is only constrained by Higgs searches at colliders. Thus, we focus on the multilepton background analyses and search strategies. This scenario can also be realized in many UV-motivated models, like in supersymmetric models [49–51] and extra-gauge symmetry such as $U(1)_{B-L}$ extended scenarios [52,53], etc., where additional constraints on the new physics sectors would apply. See Ref. [8] for a recent theory review.

The extended scalar potential would contain S self-interacting terms $V(S)$ and H, S mixing terms. We would assume a small mixing term $\lambda v_S v_H \ll m_h^2$, so that the H and S sectors minimize independently and develop their VEVs without qualitatively interfering with the electroweak breaking process. The mass matrix near the minimum can be written as

$$
\begin{array}{c|cc}
 & h & s \\
\hline
h & m_h^2 & \lambda v_H v_S, \\
s & \lambda v_H v_S & m_s^2
\end{array}
\qquad (2)
$$

where h and s are the neutral scalar modes near the minimum, with $(v_H + h)/\sqrt{2} \sim \text{Re} H^0$. m_h and m_s represent the h and s masses from H and S potentials without the mixing term. Diagonalizing into the mass eigenstates, the scalars then mix by an angle α,

$$
\begin{pmatrix} h_1 \\ h_2 \end{pmatrix} = \begin{pmatrix} \cos\alpha & -\sin\alpha \\ \sin\alpha & \cos\alpha \end{pmatrix} \begin{pmatrix} h \\ s \end{pmatrix},
\qquad (3)
$$

where h and s represent the Higgs doublet and singlet modes around their VEVs. h_1, h_2 are the physical mass eigenstates. h_1 is dominated by h and identified as the 125 GeV Higgs boson. h_2 is dominated by the singlet s, and it picks up a weakly charged h component via mixing. h_2 is subject to diphoton resonance searches [54,55], and its mass range is less stringently constrained when the mixing angle is small,

$$
\alpha = \frac{\lambda v_H v_S}{|m_s^2 - m_h^2|}.
\qquad (4)
$$

In the small mixing limit ($\lambda \to 0$), the denominator can be well approximated by $|m_s^2 - m_h^2| \sim |m_{h_1}^2 - m_{h_2}^2 + \mathcal{O}(\sin^2\alpha)|$ if the scalars are not mass degenerate. Interestingly, if h_2 resides in the mass window $2m_N < m_{h_2} < \sqrt{s} - m_Z$, the production of Zh_2 is kinematically viable and $h_2 \to NN$ decay can also contribute significantly to the signal. However, this would also require m_{h_2} to be comparable to the Higgs boson's mass when the center-of-mass energy $\sqrt{s}$ is limited, particularly so if the e^-e^+ energy is just above the Zh_1 threshold at the Higgs factory. In this work, we focus on a 240 GeV e^+e^- center-of-mass energy; we

assume m_s to be generally outside this rather narrow window and only include h_1 production.

In case m_s is much heavier than the weak scale, S can be integrated out in the Lagrangian, and the Higgs doublet can have an effective dim-5 $\bar{N}_R^C N_R H^\dagger H$ operator with a dimensionful coupling, like in νSMEFT setups [18,56], where the only h_1 decays to NN and any heavy scalars do not appear at low scale. Note that at a 240 GeV center-of-mass energy, m_s is not necessarily heavy enough for h_2 to be outside the collider's energy reach. An h_2 below ~300 GeV causes very significant h-s mixing in Eq. (4) unless $\lambda \ll 1$, so when the mass window opens up for on-shell h_2 production—e.g., at 360 GeV or higher—resonant $h_2 \to NN$ also becomes relevant, and m_{h_2} alters both the total signal rate and the kinematics of the decay products [45]. Since we are generally interested in resonant NN production through these states, we will allow S to have a weak scale mass. Our kinematic analysis and search strategies would be applicable to $h_2 \to NN$ for future lepton collision runs at 360 GeV and 500 GeV center-of-mass energies.

The $h_1 \to NN$ decay branching fraction is

$$
\text{BR}_{h_1 \to NN} = \Gamma_{h_1}^{-1} \cdot \frac{|\sin\alpha \cdot y_S|^2 m_{h_1}}{16\pi} \left(1 - \frac{4m_N^2}{m_{h_1}^2}\right)^{3/2}, \quad (5)
$$

which assumes Majorana N throughout this paper,[1] taking the total Higgs boson width as $\Gamma_{h_1} \sim 4$ MeV. We would also assume $m_N < m_{h_1}/2$ so that the heavy neutrinos are produced on shell. Note that current collider limits do not exclude a very light singlet-dominated scalar boson, $m_s \ll m_h$, which either indicates for a small v_S (requiring $\lambda \ll 1$, plus an overunity y_S for a massive N), or requires $V(S)$ to be rather flat near its minimum with a large v_S. However, a very light scalar can not on-shell decay into NN in our mass range of interest; thus, we do not consider this scenario in this analysis.

Unlike Higgs production in pp collisions, where gluon fusion dominates, the leading production channel in e^-e^+ collisions is through the s-channel Z with an associated final-state Z boson, as shown in Fig. 1. The $h_1 \to NN$ system leads to the characteristic rare Higgs decay signals with SS lepton pair(s). Here we do not include the $h_1 \to N\nu$ channel [20,23,26,57,58], as this h_1 decay to $N\nu$ occurs via the left-handed component in N, and the effective coupling is proportional to $|V_{\ell N}|^2 \sim m_\nu/m_N$. Consider the parameter range $1 \gg |\sin\alpha|^2 \gg m_\nu/m_N$, as will be shown later to be relevant to collider sensitivity limits; the $h_1 \to NN$ decay dominates over $h_1 \to N\nu$. Thus, $h_1 \to NN$ serves as a complementary search to $|V_{\ell N}|^2$-based channels in the presence of Higgs mixing with a BSM scalar.

---

[1]For Dirac-type heavy neutrinos, the differences in decay fraction and kinematics require a separate analysis on cut efficiencies.
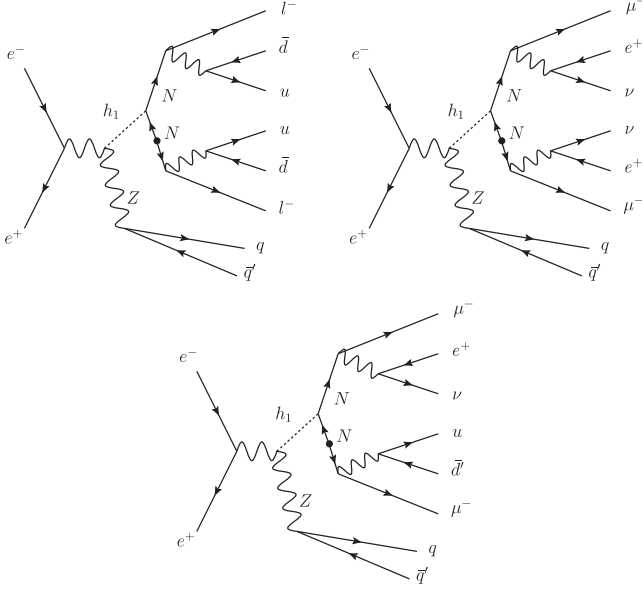
FIG. 1. Illustrative processes of SS dilepton production from semileptonic (upper-left), leptonic (upper-right), and mixed (lower) decays of the NN system.

The associated Z boson can decay to a lepton or jet pair, and their invariant mass reconstructs to m_Z. For signal selection, the decay mode of the $Z \to jj$ is favorable, as it would

  (i) demand the SM background to be also accompanied by one additional Z boson.

  (ii) remove potential lepton-number uncertainty from neutrinos in case LNV is required in the final state.

 (iii) ensure the leptons are from the NN decay.

The $h_1 \to NN$ branching fraction is proportional to $\sin^2 \alpha$. N decays through its ν_L component, and its partial width is suppressed by $|V_{\ell N}|^2$. $N \to \ell W^*$ is the dominant N-decay channel; its hadronic and leptonic $W^* \to jj, \ell\nu$ decays lead to "semileptonic" and "fully leptonic" final states; see Ref. [45] for branching fraction calculations. The $N \to \nu h_1^*, \nu Z^*$ channels are subleading, and they require missing or wrong-sign leptons to form SS dileptons.

A major SM background consists of τ-lepton or on-shell W-boson decays, where the $W\ell\nu$ vertex can couple to any lepton flavor. Same-sign and same-flavor dileptons require the presence of same-sign τ or W pairs, and charge conservation would demand four $W^{(*)}\ell\nu$ vertices in a SM final state. Opposite-sign and same-flavor dileptons arise from lepton pair production from neutral bosons, which can be vetoed by lepton charge cuts. Another background arises from wrong-sign leptons or missed leptons that can be controlled by stringent lepton cuts in event analysis. The following sections will discuss the backgrounds for each channel.

In a final state with three or more leptons, opposite-sign, same-flavor (OSSF) lepton pairs should be vetoed to suppress the SM background, which also means that at

least one SSSF lepton pair will be selected. For some signal processes, this requires N to couple to more than one lepton flavor, and we assume N couples equally to both e and μ flavors in our analysis.

In this study, we consider heavy Majorana neutrinos for all three signal channels. The two-lepton channel has no missing energy in the final state and violates lepton number apparently. A Majorana N is necessary to produce this signal. For the three- and four-lepton channels, the final state has missing energy from neutrino(s) or antineutrino(s). Since the detectors at colliders cannot identify the differences between the neutrinos and antineutrinos, the final state with missing energy can be from LNV or LNC processes. Therefore, although our analyses is for heavy Majorana N for all three signal channels, a Dirac N would also produce the three- and four-lepton signal channels. Once the heavy neutrinos are discovered from these two signal channels, more studies are needed to determine their Majorana or Dirac nature.

For convenience with collider analysis, we assume that only one heavy neutrino is kinematically accessible in h_1 decay and it couples equally to e and μ, namely $|V_{eN}| = |V_{\mu N}|$ and $V_{\tau N} = 0$. We ignore $V_{\tau N}$ in this study for two reasons: (i) the major SM background contamination is from channels with multiple τ leptons, and (ii) the additional leptonic τ decay branching further reduces the signal rate. The collider sensitivity on $V_{\tau N}$ is thus expected to be less stringent.

We perform cut-and-count analyses on Monte Carlo simulated signal and background events. For the signal simulation, the interaction terms in Eq. (1) plus the SM Lagrangian are implemented in the FeynRules program [59] to create the model file in the Universal FeynRules Output (UFO) format [60]. Events are generated by MadGraph5 [61] and showered by the PYTHIA 8 [62,63] package. τ lepton decays are handled by TAUOLA [64], as is implemented in PYTHIA 8. e^-e^+ detector simulation is performed by DELPHES [65] with CEPC parametrization [66]. At event generation level, we adopt jet cuts $\eta(j) < 5.0$, $p_T(j) > 20$ GeV and use relatively lenient lepton cuts $\eta(\ell) < 2.5$, $p_T(\ell) > 0.5$ GeV. Angular separation cuts $\Delta R(j, j)$, $\Delta R(\ell, \ell) > 0.3$ are also implemented. We note that at future lepton colliders, the p_T triggers for jets could be lower than 20 GeV. However, for the multijet final state, the reconstruction quality and efficiency will become worse when jets $p_T < 10$ GeV. Since our signals have harder p_T's for jets than the background [see, for example, the $p_T(j)$ distributions in Fig. 2], a lower threshold will lead to more background, and thus we choose 20 GeV as a benchmark analysis.

III. TWO-LEPTON CHANNEL

The $h_1 \to NN \to \ell^\pm \ell^\pm + 4j, \ell = e, \mu$ channel requires that both N's decay to a charged lepton and two jets ($W^* \to \bar{q}q'$), and that one of the N's decays as its own
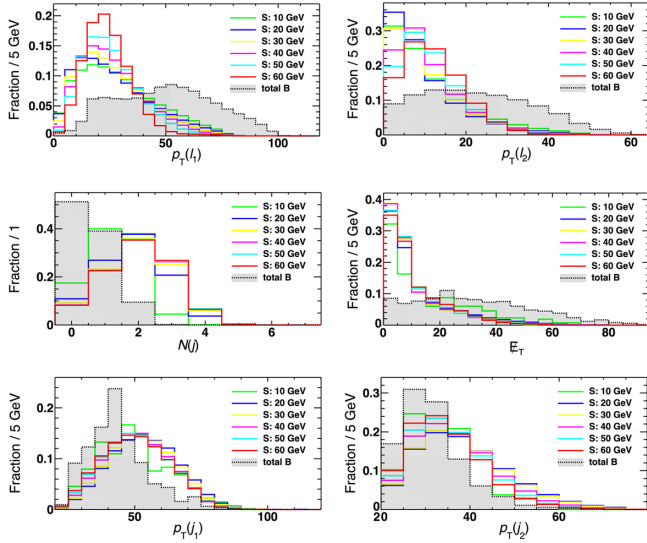
FIG. 2. Normalized distribution of selected kinematic variables to differentiate signals from the total SM background for the 2ℓ channel. $p_T(\ell)$ panels show the selection $N(l) = 2$, $N(j)$ applies cuts (i) and (ii), and $\not{E}_T$, $p_T(j)$ panels use cuts (i)–(iv).

antiparticle. This final state has no missing energy and violates lepton number with $\Delta L = 2$, and it is often considered the "smoking gun" channel of the heavy Majorana neutrino search with explicit LNV.

Note that in this channel NN decays to four jets. Unlike being easily contaminated in pp collision [67,68], the much cleaner environment in an $e^- e^+$ collision is largely free of fake leptons from soft jets. However, due to the small energy cap between the Higgs boson and heavy neutrino, these four jets are relatively soft and can be difficult to fully reconstruct. With fewer jets, wrong-sign and unreconstructed leptons become possible backgrounds,

in addition to intrinsic multiple-τ, W backgrounds. The relevant background channels are listed in Table I.

The background channels contain two or more τ leptons or light charged leptons $\ell = e, \mu$, plus Z or $W^+ W^-$, that yield dijet resonance near Z mass. The particle signs are omitted, and any even number of τ, ℓ, and W entries must include an equal number of opposite-sign particles—e.g., 4τ denotes $2\tau^+ 2\tau^-$, and $2\ell 2W$ stands for $\ell^+ \ell^- W^+ W^-$, etc. While the SM backgrounds $\ell\ell$ are restricted to same-flavor, opposite-sign lepton pairs, leptonic W decay can provide one additional lepton and create a like-sign dilepton combination in case one lepton is undetected. Such channels are marked with $\dagger$ in the table.

The signal event contains one SS dilepton, two jets from Z decay, and a number of soft jets, plus very little missing energy. We select hadronic Z decay by imposing a charged lepton number $N(\ell) = 2$ to avoid confusion between the leptons from Z decay and those from NN decay. With a jet transverse momentum requirement of $p_T(j) > 20$ GeV, the soft jets from the NN system are not always identifiable, especially when the jets are more collimated if N is light and relatively boosted. Still, having at least one extra jet in addition to those from Z can be effective in background rejection, so we consider the jet counting cut $N(j) \geq 3$.

Event selection includes the following cuts:
(i) Exactly two leptons, $N(\ell) = 2$ with $p_T(\ell) > 5$ GeV.
(ii) Two leptons with the same sign.
(iii) Veto τ leptons, $N(\tau) = 0$.
(iv) At least three jets, $N(j) \geq 3$.
(v) Small missing energy, $\not{E}_T < 15$ GeV.

The histograms of a few crucial kinetic observables for the signal with different m_N's and the total background are shown in Fig. 2. $p_T(\ell_1)$ and $p_T(\ell_2)$ correspond to the samples after requiring $N(\ell) = 2$; $N(j)$ is after selecting

TABLE I. The expected number of signal and background events for the 2ℓ channel at a future $e^- e^+$ collider with $\sqrt{s} = 240$ GeV and 5.6 ab^{-1} integrated luminosity. Signal rates assume a benchmark branching fraction BR($h_1 \rightarrow NN$) = 9.1×10^{-4}. Background channels marked with $\dagger$ require wrong-sign or missing leptons. Empty cells denote event numbers below 10^{-3}.

		Initial	Cuts (i),(ii)	Cuts (iii),(iv)	Cut (v)
Sig.	10 GeV	10^3	6.3	0.29	0.18
	20 GeV	10^3	35.9	8.8	6.4
	30 GeV	10^3	72.3	22.6	17.5
	40 GeV	10^3	97.2	32.5	25.3
	50 GeV	10^3	112	37.4	28.8
	60 GeV	10^3	121	40.5	30.2
Bkg.	4τ	1.69×10^4	870	4.6×10^{-2}	7.7×10^{-3}
	$^\dagger 2\tau Z$	6.80×10^5	2.91×10^3	4.6	0.93
	$^\dagger 2\tau Z$	1.74×10^6	3.98×10^3	$\cdots$	$\cdots$
	$4\tau Z$	93.0	2.0	0.19	5.9×10^{-2}
	$2\tau 2W$	4.42×10^3	63.6	0.92	8.2×10^{-2}
	$^\dagger 2\ell 2\tau Z$	584	13.8	2.0	0.75
	$^\dagger 4\ell Z$	862	16.5	2.2	2.1
	$^\dagger 2\ell 2W$	2.74×10^4	639	11.7	1.2

cuts (i) and (ii); and $\not{E}_T$, $p_T(j_2)$, and $p_T(j_3)$ are after requiring cuts (i)–(iv). These distributions illustrate the effectiveness of our selection cuts. The $N(j)$ cut can be very effective in background rejection, and we select $N(j) \geq 3$, as it yields the best signal significance.

Since the t-quark background is not a problem in e^-e^+ collisions, the b-jet veto is not included, but the τ veto is still helpful in removing multi-τ background events. The expected number of events at different cut stages for signal and background channels are listed in Table I. The benchmark branching fraction $\text{BR}(h_1 \to NN)$ is chosen to be 9.1×10^{-4}, so that the precut ("initial") signal event rate is around 10^3, and the signal cut efficiencies can be conveniently converted. The expected signal event number N_s with selection cuts can be calculated from Eq. (6).

The major background includes $4\ell Z$, $2\tau Z$, $2\ell 2\tau Z$, and $2\ell 2W$ channels. The $4\ell Z$ and $2\ell 2\tau Z$ channels can fake a signal by missing two final-state leptons with the same sign. In the $2\ell 2W$ channel, $W \to jj$ provides the required jets, and one missed lepton with the opposite sign can result in a fake signal event. As shown in Table I, these channels contribute more background events than the "intrinsic" $4\tau Z$ channel, and this shows the complication with selecting only one pair of same-sign leptons. The $2\tau Z$ background events are likely from one wrong-sign lepton.

IV. THREE-LEPTON CHANNEL

When one N decays leptonically and the other N decays semileptonically, the three leptons in the final state $Zh_1 \to \ell^\pm \ell^\pm \ell + 4j + \not{E}_T$ may contain one SSSF dilepton combination. Compared to the 2ℓ channel, the SSSF dilepton signal occurs with both lepton-number-violating ($\Delta L = 2$) and lepton-number-conserving ($\Delta L = 0$) decays of NN. The $\Delta L = 2$ process is shown in Fig. 1. When N couples to at least two lepton flavors (e.g., to both e and μ), the $\Delta L = 0$ process can also obtain the same-sign lepton from the secondary leptonic $W^* \to \ell\nu$ vertex instead of the primary $N \to \ell W$ vertex, and thus this signal does not confirm that N is Majorana-type.

Similarly to the 2ℓ channel, the SM background includes channels with multiple τ and W bosons. The OSSF lepton pair (e.g., $e^\pm e^\mp$) should be vetoed to suppress the SM background.

We select signal events with the following cuts:

(i) Exactly three leptons $N(\ell) = 3$ with $p_T \geq 5$ GeV.
(ii) Veto OSSF lepton pairs.
(iii) Veto τ leptons, $N(\tau) = 0$.
(iv) At least two jets, $N(j) \geq 2$.

The distributions of selected kinetic variables in the 3ℓ channel are shown in Fig. 3. $p_T(\ell_1)$, $p_T(\ell_2)$, and $p_T(\ell_3)$ correspond to the samples after requiring $N(\ell) = 3$; $N(j)$ is after selecting cuts (i) and (ii); and $p_T(j_1)$ and $p_T(j_2)$ are after requiring cuts (i)–(iv). The $N(j)$ cut is selected to optimize the signal significance.
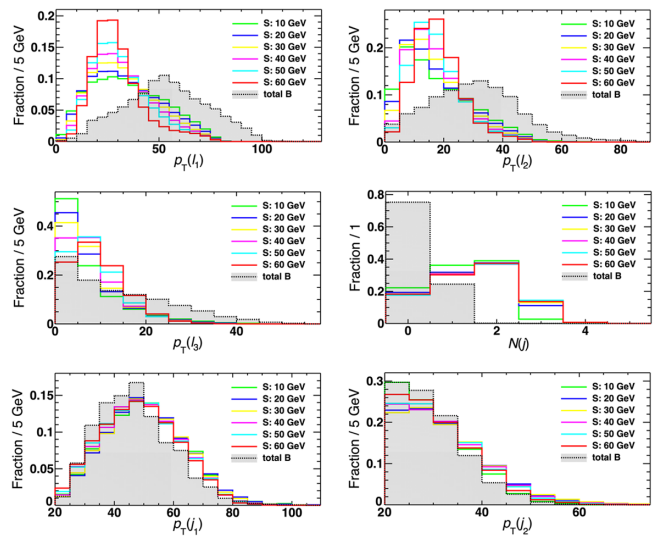

FIG. 3. Normalized distribution of selected kinematic variables for the 3ℓ channel. $p_T(\ell)$ panels show the selection $N(l) = 3$, $N(j)$ applies cuts (i) and (ii), and $p_T(j)$ panels use cuts (i)–(iv).

Table II lists the expected number of events at different cut stages for a signal with different N masses and background channels. In clear contrast to the 2ℓ channel, the surviving backgrounds are $2\tau 2W$ and $2\tau 2lZ$ channels. The combination of the $N(j)$ cut and the increased lepton number cut effectively removes the background from leptonic W decays, which leads to a smaller total background event rate. Because of both a lower leptonic N decay branching fraction and fewer jets from NN decays, the signal event rate is also lower compared to the 2ℓ channel.

Interestingly, selecting three leptons will pick up a same-sign *trilepton* final state of $\ell^\pm \ell^\pm \ell^\pm$ that derives from leptonic Z decay, as shown in Fig. 4. The jets from semileptonic NN decay satisfy the jet cuts, and $\ell^\pm \ell^\pm \ell^\pm$ emerges once the opposite-sign $\ell^\mp$ misses detection. Among $\ell^\pm \ell^\pm \ell^\pm$ events, a fraction of $\frac{1}{2}(x_e^2 + x_\mu^2)/\sum_{\ell,\ell'} x_\ell x_{\ell'}$ have the same flavor for all three leptons (i.e., SSSF trilepton $e^\pm e^\pm e^\pm$ and $\mu^\pm \mu^\pm \mu^\pm$), where $x_{\ell=e,\mu}$ denotes the branching fraction of N decay into each lepton flavor that is proportional to $|V_{\ell N}|^2$. At our choice of $x_e : x_\mu = 1:1$, one quarter of the SS trileptons have the same flavor.

At $m_N = 60$ GeV, this same-charge trilepton final state $\ell^\pm \ell^\pm \ell^\pm$ is 7.6% of the $\ell^\pm \ell^\pm \ell$ signal events after selecting cuts (i) and (ii). In comparison, SM events would need at least three missed or wrong-sign leptons to fake such a process. The SSSF trilepton background rate is found to be about 0.1% of the original 3ℓ background event rate after cuts (i) and (ii). If capped by luminosity limits, SSSF trilepton signal does not necessarily yield stronger sensitivity, as its expected signal event rate is small.

TABLE II. Similar to Table I, but for the 3ℓ channel. Background channels with † require missing leptons.

		*Initial	Cut (i)	Cut (ii)	Cuts (iii),(iv)
Sig.	10 GeV	10^3	27.9	5.6	2.3
	20 GeV	10^3	62.7	13.6	6.6
	30 GeV	10^3	85.8	19.9	10.0
	40 GeV	10^3	102	24.9	12.7
	50 GeV	10^3	112	27.3	14.1
	60 GeV	10^3	115	28.2	14.4
Bkg.	4τ	1.69×10^4	614	155	3.8×10^{-2}
	$^\dagger 2\tau Z$	6.80×10^5	1.30×10^4	350	$\cdots$
	$^\dagger 2\ell Z$	1.74×10^6	5.03×10^4	121	$\cdots$
	$4\tau Z$	93.0	2.1	0.25	7.3×10^{-2}
	$2\tau 2W$	4.42×10^3	27.8	6.9	0.72
	$^\dagger 2\ell 2\tau Z$	584	46.5	1.1	0.44
	$^\dagger 4\ell Z$	862	132	0.27	1.4×10^{-2}
	$^\dagger 2\ell 2W$	2.74×10^4	1.30×10^3	37.8	5.0×10^{-2}

V. FOUR-LEPTON CHANNEL

The fully leptonic NN decay leads to four charged leptons. When N couples to both the first and second lepton generations, two SSSF dileptons $e^\pm e^\pm \mu^\mp \mu^\mp$ can emerge, and the two pairs must be in different flavors to avoid the OSSF dilepton pairs. Due to the presence of (anti)neutrinos, this final state does not guarantee LNV, and it receives contributions from both LNV and non-LNV decays of N. Therefore, similarly to Sec. IV, this signal does not require that N must be Majorana.

The fully leptonic branching fraction is lower than the semileptonic branching fraction due to the smaller leptonic $W^* \to l\nu$ branching compared to the hadronic $W^* \to jj$ branching, plus the requirement that the two dileptons must differ in flavor. Having two SSSF dileptons can provide *major* reduction on backgrounds, and it is shown that the SM background can be below the single-event level in pp collisions [45]. With $e^- e^+$ collisions, an even lower background is expected, and it would be interesting to investigate at what luminosity level the background becomes relevant.
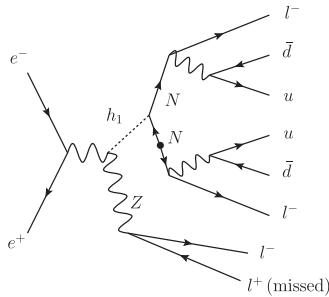
Similarly to the semileptonic case, the SM background arises from multiple τ, W channels with one associated Z boson. We consider the following selection cuts in event analysis:

(i) Exactly four leptons, $N(\ell) = 4$ with $p_T(\ell) \geq 5$ GeV.
(ii) Exactly two electrons with the same charges, and exactly two muons with the same charges; the electrons and muons have opposite charges—i.e., exactly $e^\pm e^\pm \mu^\mp \mu^\mp$ lepton pairs.
(iii) Veto τ leptons, $N(\tau) = 0$.
(iv) At least one jet, $N(j) \geq 1$.

The kinetic distributions of selected observables for the signal with different N masses and the total background are shown in Fig. 5. $p_T(\ell_1)$, $p_T(\ell_2)$, $p_T(\ell_3)$, $p_T(\ell_4)$
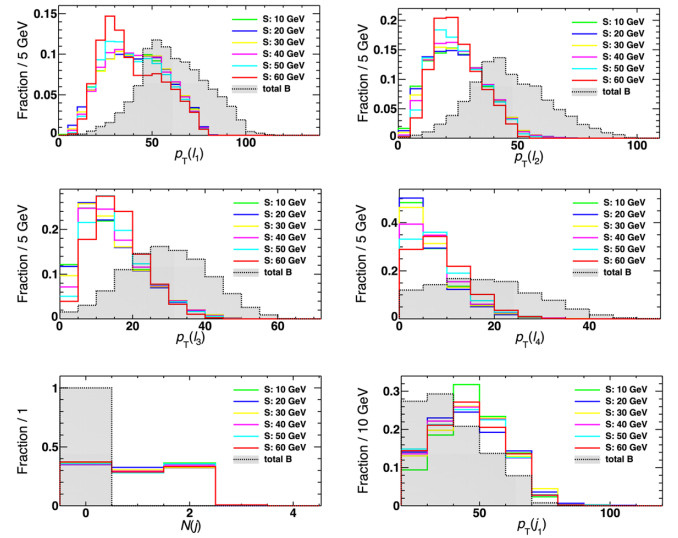

FIG. 5. Normalized distribution of selected kinematic variables for the 4ℓ channel. $p_T(\ell)$ panels show the selection $N(l) = 4$, $N(j)$ applies cuts (i) and (ii), and $p_T(j)$ panels use cuts (i)–(iv).

FIG. 4. The SS trilepton emerges when Z decays leptonically and the opposite-sign lepton misses detection.

TABLE III. Similar to Table I, but for the 4ℓ channel. Background channels with $\dagger$ require missing leptons or wrong signs.

		Initial	Cut (i)	Cut (ii)	Cuts (iii),(iv)
Sig.	10 GeV	10^3	15.9	1.1	0.71
	20 GeV	10^3	17.5	1.1	0.72
	30 GeV	10^3	22.1	1.3	0.80
	40 GeV	10^3	26.8	1.5	0.98
	50 GeV	10^3	30.1	1.8	1.2
	60 GeV	10^3	32.1	2.1	1.3
Bkg.	4τ	1.69×10^4	58.4	6.8	$\cdots$
	$^\dagger 2\tau Z$	6.80×10^5	2.26×10^3	9.6	$\cdots$
	$^\dagger 2\ell Z$	1.74×10^6	7.28×10^4	$\cdots$	$\cdots$
	$4\tau Z$	93.0	0.45	6.4×10^{-3}	2.8×10^{-3}
	$2\tau 2W$	4.42×10^3	1.3	0.17	$\cdots$
	$^\dagger 2\ell 2\tau Z$	584	13.8	1.0×10^{-2}	3.2×10^{-3}
	$^\dagger 4\ell Z$	862	116	7.8×10^{-4}	$\cdots$
	$^\dagger 2\ell 2W$	2.74×10^4	217	$\cdots$	$\cdots$

correspond to the samples after requiring $N(\ell) = 4$; $N(j)$ is after selecting cuts (i) and (ii); and $p_T(j_1)$ is after requiring cuts (i)–(iv).

The expected numbers of events at different cut stages for signals with different N masses and background channels are shown in Table III. Due to two SSSF dileptons, two wrong-sign leptons must occur to fake such an event. Missing leptons are also less of a problem, as it would take a $2\tau 2e2\mu Z$ final state with one missed e and one missed μ to fake the signal.

The surviving backgrounds are the $4\tau Z$ and $2\ell 2\tau Z$ channels. The lepton flavor and opposite-sign cuts play the central role in rejecting the background with same-flavor, opposite-sign leptons. Stringent lepton counting removes the background from hadronic τ decays. The $2\tau 2\ell Z$ channel still contributes to background events, possibly due to wrong-sign leptons.

VI. RESULTS

Signal event samples are generated with the $e^- e^+ \to Z h_1 \to Z(NN)$ process, and then we let the Z boson and the heavy neutrinos decay inclusively. The signal event rate is

$$N_s = L \cdot \sigma_{Z h_1} \cdot \mathrm{BR}(h_1 \to NN) \cdot \eta_s, \qquad (6)$$

where L is the collider luminosity and η_s denotes the cut-based selection efficiency on the generated signal events. With a design luminosity $L = 5.6$ ab^{-1} and $\sigma_{Z h_1} = 196$ fb at 240 GeV center-of-mass energy [36], a sample of 1.1×10^6 $Z h_1$ events is expected. Since we let N decay inclusively, η_s already includes the NN system's combined branching fraction into the selected final states, thus the formula above does not explicitly contain the N decay branching fraction. The signal's statistic significance is

$$\sigma_{\mathrm{stat}} = \sqrt{2\left[(N_s + N_b) \ln\left(1 + \frac{N_s}{N_b}\right) - N_s\right]}. \qquad (7)$$

The background event rates N_b for the 2ℓ, 3ℓ, and 4ℓ channels are listed in Tables I–III, respectively. Requiring 2σ and 5σ significance levels, the sensitivity limits on $\mathrm{BR}(h_1 \to NN)$ are shown in Fig. 6.

Given $L \cdot \sigma_{Z h_1} \sim 10^6$, the $\mathrm{BR}(h_1 \to NN)\, \eta_s$ combination in Eq. (6) is statistically limited by $N_s / N_{Z h_1} \sim 10^{-6} N_s$. The selection efficiency η_s is favorably evaluated via Monte Carlo, as η_s is weighted between different decay chains that contribute to the same final state. In our case, $Z \to \ell\ell, jj$ both contribute to the signal channels.

Note that 2ℓ and 3ℓ limits worsen towards lower m_N. This is caused by N decaying into collimated leptons and jets when N becomes more boosted at smaller m_N, resulting in fewer and softer reconstructed jets; hence, it is hard hit by the jet selection cuts. Relaxing the jet cuts would help in recovering more low-m_N signal events, yet at the cost of
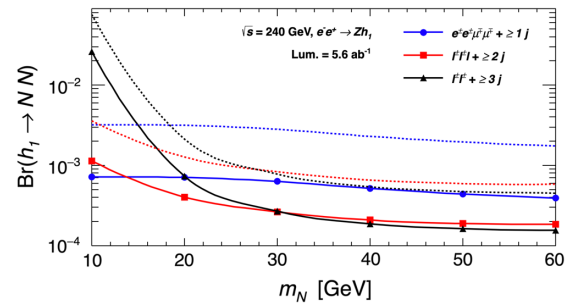

FIG. 6. Sensitivity limits on the decay branching ratio of Higgs boson to NN for 2ℓ–4ℓ channels, assuming an m_N between 10 and 60 GeV. $Z h_1$ production assumes a 240 GeV center-of-mass energy and 5.6 ab^{-1} integrated luminosity at future $e^- e^+$ colliders. The solid (dotted) curves correspond to 2σ (5σ) significance.

significantly increasing the SM background. The 4ℓ channel has the highest background veto efficiency that can saturate the luminosity cap ($N_b < 1$) up to 10^3 ab^{-1}. Despite the subunity background event rate, the 4ℓ channel's sensitivity is less stringent than the 2ℓ and 3ℓ channels' for larger m_N because of its much lower signal selection efficiency.

BR($h_1 \to NN$) relates to BSM parameters as

$$|\sin\alpha \cdot y_S|^2 = \mathrm{BR}(h_1 \to NN)$$
$$\times 16\pi \frac{\Gamma_{h_1}}{m_{h_1}} \left(1 - \frac{4m_N^2}{m_{h_1}^2}\right)^{-3/2}. \tag{8}$$

A BR($h_1 \to NN$) $= 10^{-4}$ sensitivity limit would correspond to $|\sin\alpha \cdot y_S|^2 \leq 7.3 \times 10^{-6}$ at $m_N = 60$ GeV, or $\leq 1.6 \times 10^{-7}$ towards low N mass $2m_N \ll m_{h_1}$, where the decay phase space is least suppressed by the mass gap as $(1 - \frac{4m_N^2}{m_{h_1}^2}) \to 1$ in Eq. (8).

y_S is a free model parameter given by v_S and m_N. For $y_S \sim \mathcal{O}(1)$, this limit constrains $|\sin\alpha|$ to be lower than 10^{-2}. This shows that the future Higgs factory has good sensitivity to tiny effective mixing angles between the Higgs boson and the BSM singlet scalar, which is comparable to the projected $|\sin\alpha|^2 \sim 10^{-4}$ sensitivity at the LHC [45].

[1] P. Minkowski, $\mu \to e\gamma$ at a rate of one out of 10^9 muon decays?, Phys. Lett. **67B,** 421 (1977).

[2] T. Yanagida, Horizontal gauge symmetry and masses of neutrinos, Conf. Proc. **C7902131,** 95 (1979).

[3] R. N. Mohapatra and G. Senjanovic, Neutrino Mass and Spontaneous Parity Nonconservation, Phys. Rev. Lett. **44,** 912 (1980).

[4] S. L. Glashow, The future of elementary particle physics, NATO Sci. Ser. B **61,** 687 (1980).

[5] M. Gell-Mann, P. Ramond, and R. Slansky, Complex spinors and unified theories, Conf. Proc. **C790927,** 315 (1979).

[6] A. Atre, T. Han, S. Pascoli, and B. Zhang, The search for heavy Majorana neutrinos, J. High Energy Phys. 05 (2009) 030.

[7] F. F. Deppisch, P. S. Bhupal Dev, and A. Pilaftsis, Neutrinos and collider physics, New J. Phys. **17,** 075019 (2015).

[8] Y. Cai, T. Han, T. Li, and R. Ruiz, Lepton number violation: Seesaw models and their collider tests, Front. Phys. **6,** 40 (2018).

[9] A. M. Sirunyan *et al.* (CMS Collaboration), Search for Heavy Neutral Leptons in Events with Three Charged Leptons in Proton-Proton Collisions at $\sqrt{s} = 13$ TeV, Phys. Rev. Lett. **120,** 221801 (2018).

[10] A. M. Sirunyan *et al.* (CMS Collaboration), Search for heavy Majorana neutrinos in same-sign dilepton channels in proton-proton collisions at $\sqrt{s} = 13$ TeV, J. High Energy Phys. 01 (2019) 122.

[11] C. Ahdida *et al.* (SHiP Collaboration), Sensitivity of the SHiP experiment to heavy neutral leptons, J. High Energy Phys. 04 (2019) 077.

[12] G. Aad *et al.* (ATLAS Collaboration), Search for heavy neutral leptons in decays of W bosons produced in 13 TeV pp collisions using prompt and displaced signatures with the ATLAS detector, J. High Energy Phys. 10 (2019) 265.

[13] R. Aaij *et al.* (LHCb Collaboration), Search for heavy neutral leptons in $W^+ \to \mu^+\mu^\pm$ jet decays, Eur. Phys. J. C **81,** 248 (2021).

[14] CMS Collaboration, Search for long-lived heavy neutral leptons with displaced vertices in pp collisions at $\sqrt{s} = 13$ TeV with the CMS detector, Report No. CMS-PAS-EXO-20-009, 2021.

[15] S. Antusch and O. Fischer, Testing sterile neutrino extensions of the Standard Model at the Circular Electron Positron Collider, Int. J. Mod. Phys. A **30,** 1544004 (2015).

[16] S. Antusch and O. Fischer, Testing sterile neutrino extensions of the Standard Model at future lepton colliders, J. High Energy Phys. 05 (2015) 053.

[17] S. Antusch, E. Cazzato, and O. Fischer, Sterile neutrino searches at future $e^- e^+$, pp, and $e^- p$ colliders, Int. J. Mod. Phys. A **32,** 1750078 (2017).

[18] D. Barducci, E. Bertuzzo, A. Caputo, P. Hernandez, and B. Mele, The see-saw portal at future Higgs Factories, J. High Energy Phys. 03 (2021) 117.

[19] W. Liao and X.-H. Wu, Signature of heavy sterile neutrinos at CEPC, Phys. Rev. D **97,** 055005 (2018).

[20] J.-N. Ding, Q. Qin, and F.-S. Yu, Heavy neutrino searches at future Z-factories, Eur. Phys. J. C **79,** 766 (2019).

[21] A. Blondel, A. de Gouvêa, and B. Kayser, Z-boson decays into Majorana or Dirac heavy neutrinos, Phys. Rev. D **104,** 055027 (2021).

[22] T. Asaka and H. Ishida, Lepton number violation by heavy Majorana neutrino in B decays, Phys. Lett. B **763**, 393 (2016).

[23] S. Banerjee, P. S. B. Dev, A. Ibarra, T. Mandal, and M. Mitra, Prospects of heavy neutrino searches at future lepton colliders, Phys. Rev. D **92**, 075002 (2015).

[24] Y. Zhang and B. Zhang, A potential scenario for Majorana neutrino detection at future lepton colliders, J. High Energy Phys. 02 (2019) 175.

[25] S. Antusch, E. Cazzato, and O. Fischer, Displaced vertex searches for sterile neutrinos at future lepton colliders, J. High Energy Phys. 12 (2016) 007.

[26] Z. S. Wang and K. Wang, Physics with far detectors at future lepton colliders, Phys. Rev. D **101**, 075046 (2020).

[27] C. O. Dib, J. C. Helo, M. Nayak, N. A. Neill, A. Soffer, and J. Zamora-Saa, Searching for a sterile neutrino that mixes predominantly with ν_τ at B factories, Phys. Rev. D **101**, 093003 (2020).

[28] A. Abada, V. De Romeri, S. Monteil, J. Orloff, and A. M. Teixeira, Indirect searches for sterile neutrinos at a high-luminosity Z-factory, J. High Energy Phys. 04 (2015) 051.

[29] J. Baglio, S. Pascoli, and C. Weiland, W^+W^-H production at lepton colliders: A new hope for heavy neutral leptons, Eur. Phys. J. C **78**, 795 (2018).

[30] A. M. Sirunyan et al. (CMS Collaboration), Search for high-mass resonances in dilepton final states in proton-proton collisions at $\sqrt{s} = 13$ TeV, J. High Energy Phys. 06 (2018) 120.

[31] G. Aad et al. (ATLAS Collaboration), Search for new resonances in mass distributions of jet pairs using 139 fb^{-1} of pp collisions at $\sqrt{s} = 13$ TeV with the ATLAS detector, J. High Energy Phys. 03 (2020) 145.

[32] P. Langacker, The physics of heavy Z' gauge bosons, Rev. Mod. Phys. **81**, 1199 (2009).

[33] E. Akhmedov, A. Kartavtsev, M. Lindner, L. Michaels, and J. Smirnov, Improving electro-weak fits with TeV-scale sterile neutrinos, J. High Energy Phys. 05 (2013) 081.

[34] L. Di Luzio, R. Gröber, and M. Spannowsky, Maxi-sizing the trilinear Higgs self-coupling: How large could it be?, Eur. Phys. J. C **77**, 788 (2017).

[35] B. Di Micco, M. Gouzevitch, J. Mazzitelli, and C. Vernieri, Higgs boson potential at colliders: Status and perspectives, Rev. Phys. **5**, 100045 (2020).

[36] M. Dong et al. (CEPC Study Group), CEPC conceptual design report: Volume 2—Physics & detector, Reports No. IHEP-CEPC-DR-2018-02, No. IHEP-EP-2018-01, No. IHEP-TH-2018-01, 2018.

[37] D. Wyler and L. Wolfenstein, Massless neutrinos in left-right symmetric models, Nucl. Phys. **B218**, 205 (1983).

[38] P. Fayet, Supergauge invariant extension of the Higgs mechanism and a model for the electron and its neutrino, Nucl. Phys. **B90**, 104 (1975).

[39] M. L. Graesser, Broadening the Higgs boson with right-handed neutrinos and a higher dimension operator at the electroweak scale, Phys. Rev. D **76**, 075006 (2007).

[40] K. Belotsky, D. Fargion, M. Khlopov, R. Konoplich, and K. Shibaev, Invisible Higgs boson decay into massive neutrinos of fourth generation, Phys. Rev. D **68**, 054027 (2003).

[41] I. M. Shoemaker, K. Petraki, and A. Kusenko, Collider signatures of sterile neutrinos in models with a gauge-singlet Higgs, J. High Energy Phys. 09 (2010) 060.

[42] A. Maiezza, M. Nemevšek, and F. Nesti, Lepton Number Violation in Higgs Decay at LHC, Phys. Rev. Lett. **115**, 081802 (2015).

[43] M. Nemevšek, F. Nesti, and J. C. Vasquez, Majorana Higgses at colliders, J. High Energy Phys. 04 (2017) 114.

[44] S. Moretti, C. H. Shepherd-Themistocleous, and H. Waltari, Lepton number violation in heavy Higgs boson decays to sneutrinos, Phys. Rev. D **101**, 015018 (2020).

[45] Y. Gao, M. Jin, and K. Wang, Probing the decoupled seesaw scalar in rare Higgs decay, J. High Energy Phys. 02 (2020) 101.

[46] CEPC Study Group, CEPC conceptual design report: Volume 1—Accelerator, Reports No. IHEP-CEPC-DR-2018-01, No. IHEP-AC-2018-01, 2018.

[47] H. Baer, T. Barklow, K. Fujii, Y. Gao, A. Hoang, S. Kanemura, J. List, H. E. Logan, A. Nomerotski, M. Perelstein et al., The international linear collider technical design report: Volume 2—Physics, Reports No. ILC-REPORT-2013-040, No. ANL-HEP-TR-13-20, No. BNL-100603-2013-IR, No. IRFU-13-59, No. CERN-ATS-2013-037, No. COCKCROFT-13-10, No. CLNS-13-2085, No. DESY-13-062, No. FERMILAB-TM-2554, No. IHEP-AC-ILC-2013-001, No. INFN-13-04-LNF, No. JAI-2013-001, No. JINR-E9-2013-35, No. JLAB-R-2013-01, No. KEK-REPORT-2013-1, No. KNU-CHEP-ILC-2013-1, No. LLNL-TR-635539, No. SLAC-R-1004, No. ILC-HIGRADE-REPORT-2013-003, 2013 [arXiv:1306 .6352].

[48] A. Abada et al. (FCC Collaboration), FCC-ee: The lepton collider: Future circular collider conceptual design report Volume 2, Eur. Phys. J. Special Topics **228**, 261 (2019).

[49] J. Cao, J. Li, Y. Pan, L. Shang, Y. Yue, and D. Zhang, Bayesian analysis of sneutrino dark matter in the NMSSM with a type-I seesaw mechanism, Phys. Rev. D **99**, 115033 (2019).

[50] R. Allahverdi, S. S. Campbell, B. Dutta, and Y. Gao, Dark matter indirect detection signals and the nature of neutrinos in the supersymmetric $U(1)_{B-L}$ extension of the Standard Model, Phys. Rev. D **90**, 073002 (2014).

[51] S. Ma, K. Wang, and J. Zhu, Higgs decay to light (pseudo) scalars in the semi-constrained NMSSM, Chin. Phys. C **45**, 023113 (2021).

[52] F. F. Deppisch, W. Liu, and M. Mitra, Long-lived heavy neutrinos from Higgs decays, J. High Energy Phys. 08 (2018) 181.

[53] S. Amrith, J. M. Butterworth, F. F. Deppisch, W. Liu, A. Varma, and D. Yallup, LHC constraints on a $B - L$ gauge model using CONTUR, J. High Energy Phys. 05 (2019) 154.

[54] A. M. Sirunyan et al. (CMS Collaboration), Search for a Standard Model-like Higgs boson in the mass range between 70 and 110 GeV in the diphoton final state in proton-proton collisions at $\sqrt{s} = 8$ and 13 TeV, Phys. Lett. B **793**, 320 (2019).

[55] V. Khachatryan et al. (CMS Collaboration), Search for diphoton resonances in the mass range from 150 to 850 GeV in pp collisions at $\sqrt{s} = 8$ TeV, Phys. Lett. B **750**, 494 (2015).

[56] A. Caputo, P. Hernandez, J. Lopez-Pavon, and J. Salvado, The seesaw portal in testable models of neutrino masses, J. High Energy Phys. 06 (2017) 112.

[57] A. Das, Y. Gao, and T. Kamon, Heavy neutrino search via the Higgs boson at the LHC, Eur. Phys. J. C **79,** 424 (2019).

[58] A. Das, P. S. B. Dev, and C. S. Kim, Constraining sterile neutrinos from precision Higgs data, Phys. Rev. D **95,** 115013 (2017).

[59] A. Alloul, N. D. Christensen, C. Degrande, C. Duhr, and B. Fuks, FeynRules 2.0: A complete toolbox for tree-level phenomenology, Comput. Phys. Commun. **185,** 2250 (2014).

[60] C. Degrande, C. Duhr, B. Fuks, D. Grellscheid, O. Mattelaer, and T. Reiter, UFO: The Universal FeynRules Output, Comput. Phys. Commun. **183,** 1201 (2012).

[61] J. Alwall, R. Frederix, S. Frixione, V. Hirschi, F. Maltoni, O. Mattelaer, H.-S. Shao, T. Stelzer, P. Torrielli, and M. Zaro, The automated computation of tree-level and next-to-leading order differential cross sections, and their matching to parton shower simulations, J. High Energy Phys. 07 (2014) 079.

[62] T. Sjostrand, S. Mrenna, and P. Z. Skands, PYTHIA 6.4 physics and manual, J. High Energy Phys. 05 (2006) 026.

[63] T. Sjostrand, S. Mrenna, and P. Z. Skands, A brief introduction to PYTHIA 8.1, Comput. Phys. Commun. **178,** 852 (2008).

[64] S. Jadach, Z. Was, R. Decker, and J. H. Kuhn, The tau decay library TAUOLA: Version 2.4, Comput. Phys. Commun. **76,** 361 (1993).

[65] J. de Favereau, C. Delaere, P. Demin, A. Giammanco, V. Lemaître, A. Mertens, and M. Selvaggi (DELPHES 3 Collaboration), DELPHES 3, A modular framework for fast simulation of a generic collider experiment, J. High Energy Phys. 02 (2014) 057.

[66] C. Chen et al., Fast simulation of the CEPC detector with DELPHES, arXiv:1712.09517.

[67] C. O. Dib, C. S. Kim, and K. Wang, Signatures of Dirac and Majorana sterile neutrinos in trilepton events at the LHC, Phys. Rev. D **95,** 115020 (2017).

[68] S. Antusch, E. Cazzato, O. Fischer, A. Hammad, and K. Wang, Lepton flavor violating dilepton dijet signatures from sterile neutrinos at proton colliders, J. High Energy Phys. 10 (2018) 067.